

Re-entrant transition of aluminum-crosslinked partially hydrolyzed polyacrylamide in a high salinity solvent by rheology and NMR

Abduljelil Sultan Kedir,^{1,2} John Georg Seland,² Arne Skauge,¹ Tormod Skauge¹

¹Uni Research, Realfagbygget, Centre for Integrated Petroleum Research (CIPR), Allégaten 41, Bergen 5007, Norway

²Department of Chemistry, University of Bergen, Realfagbygget, Allégaten 41, Bergen 5007, Norway

Correspondence to: A. S. Kedir (E-mail: abduljelil.kedir@uni.no)

ABSTRACT: Linked polymer solution (LPS) is a nanoparticle polymer and designed by crosslinking a high molecular weight partially hydrolyzed polyacrylamide (HPAM) with aluminum (III). It has been applied in the oil industry to enhance oil recovery by improving sweep efficiency and by microscopic diversion in porous media. To achieve good propagation properties, aggregates formed by intermolecular crosslinking and gel formation should be avoided. To our knowledge, there is no established method to distinguish between intra- and intermolecular crosslinking for high molecular weight ($>10 \times 10^6$ Da), low concentration (<1000 ppm), polydisperse solutions of partially hydrolyzed polyacrylamides in high salinity solvents (5 wt % NaCl). The high salinity solvent is relevant to represent for formation water in many oil reservoirs. The main objective of the present study is to establish an experimental method for determining phase transition of LPS from monomeric coiled state to aggregated state in a high salinity solvent. No single experimental methods are conclusive and we have therefore applied a combinatorics approach including two-dimensional NMR, dynamic rheology, and UV spectroscopy. The different techniques show similar trends, which allow overall interpretations of phase transitions to be made. The experimental results indicated that the LPS solution at high salinity solvent underwent a phase transition by chain re-expansion, called reentrant transition. The transition point was observed at addition of 100 ppm of Al^{3+} . Higher concentrations of Al^{3+} suppressed the rate of reentrant transition, most likely because of intramolecular crosslinking of HPAM chains by Al^{3+} . Intermolecular crosslinking reaction was not observed at these conditions. © 2016 Wiley Periodicals, Inc. *J. Appl. Polym. Sci.* **2016**, *133*, 43825.

KEYWORDS: nanostructured polymers; oil and gas; spectroscopy; supramolecular structures; viscosity and viscoelasticity

Received 28 January 2016; accepted 25 April 2016

DOI: 10.1002/app.43825

INTRODUCTION

Interest in nanoparticle applications has been stimulated in the oil and gas industry in recent years. One of the applications is to use nanoparticles as flooding agents to enhance oil recovery. Linked polymer solution (LPS) is one of the nanoparticles (hydrodynamic radius ~ 150 nm) that have been used as flooding agent to enhance oil recovery.¹ It is formulated by low concentration of partially hydrolyzed polyacrylamide (HPAM) and aluminum citrate (AlCit). Injection of LPS into the porous media may improve oil recovery by increase the solution viscosity (improve sweep efficiency) and by temporary blocking of narrow pores (microscopic diversion). LPS has been implemented successfully in onshore fields in China.^{2–5} Laboratory core floods experiments have shown increased oil recovery of 20–60%.¹ However, to improve application of LPS at various reservoir temperatures and formation water salinities, more

detailed knowledge is needed with regard to conformational state and phase transitions of these nanoparticles. In this paper we limit the term “phase transition” to describe molecular chain expansion and contraction of the polymer. LPS experiences conformational changes depending on polymer concentration, crosslinker concentration, salinity, pH, and temperature.

Partially hydrolyzed polyacrylamide (HPAM) is polyelectrolyte macromolecule with flexible chain and good solubility in water. In deionized water, HPAM exhibit random and expanded conformational state because of electrostatic repulsion between charged monomer units. However, in the presence of counterions the charge density of HPAM can be reduced as result of ion–ion and ion–dipole interactions. This interplay modifies the electrostatic interactions and restricts the randomness and flexibility of polymer chains. The degree of chain flexibility depends not only on electrostatic interactions, but also the counterion

Additional Supporting Information may be found in the online version of this article.

© 2016 Wiley Periodicals, Inc.

distribution. Aluminum (III) is a multivalent counterion and affects the average chain conformation and molecular mobility of HPAM via counterion condensation and ionic bonding.

Polyelectrolytes undergo coil-to-globule transition depending on the ionic strength of solution. In very low salinity solvents, the Debye screening length is greater than the chain size and thereby there is a weak electrostatic interaction between polymer and counterions. However, the polymer chains have tendency to swell because of osmotic pressures inside the polymer is higher than bulk solution, osmotic swelling.⁶ Steady increase in salinity tends to compact the polymer chain due to screening of repulsion forces and develops a globule state, resulting in a coil-to-globule transition. In saline solution, if the distance between charged monomer units is larger than the Debye screening length, the strength of repulsion force between monomer units decreases exponentially. However, if this distance is smaller than Debye screening length, there is still interaction through the unscreened Coulomb potential that result in local chain stretching and stiffening.⁷ Multivalent counterions compact polymer chains more than monovalent counterions due to screening of the electrostatic repulsion through counterion condensation and ionic bonding.

In very high salinity solvents, the polymer backbone chain undergoes another phase transition from globule to extended state, called reentrant swelling or redissolution. This essential behavior of polyelectrolyte has drawn substantial attention in theoretical and experimental studies that is found in, e.g., DNA^{8–10}, DNA–liposome interactions,¹¹ proteins,^{12,13} dilute linear polyelectrolytes,^{14–19} and polyelectrolyte gels.^{6,20} The reentrant transition occurs due to charge inversion of polyelectrolytes, and is verified by electrophoretic mobility measurements.⁸ A number of mechanisms have been proposed to explain the charge inversion induced by mono- and multivalent counterions. Among these, a concentrated saline solution induced overcharging of the original charge of polyelectrolyte that leads to charge inversion of the polyelectrolyte.^{14,17,21} Counterion association is another hypothesis in which counterions associate with their co-ions at high salinity as result of entropic and steric effects and leads to the polyelectrolyte re-gaining charge.^{15,22} On the contrary, Hsiao studied polyelectrolytes with tetravalent counterions by theoretical and electrophoresis experiments. The results showed that the polyelectrolyte experiences chain re-expansion, but not necessarily by charge inversion. However, charge inversion can occur only when the size of multivalent counterions are small.

Many of the reentrant swelling studies are theoretical and simulation, probably because experimental methods have limitations for dilute polyelectrolyte solutions and highly saline solvents.²³ Only few experimental works have been reported on the reentrant transition of polyelectrolytes, e.g., sodium poly(styrenesulfonate) studied by theoretical and light scattering measurement,²⁴ particle tracking microrheology,²² fluorescence correlation spectroscopy²⁵ and quartz crystal microbalance with dissipation²⁶ in the presence of multivalent counterions. This polymer was studied by small-angle neutron scattering at high ionic strength and the result showed that the chain appears to be thicker, presumably due to reentrant swelling.²⁷ Experimental studies conducted on

poly(2-vinylpyridine)^{23,28} and poly(*N*-methyl-2-vinylpyridinium iodide)²⁸ in the presence of mono- and multivalent counterions demonstrated chain collapse and reentrant transition. Theoretical studies predicted that the degree of chain re-expansion by multivalent ions is stronger than monovalent ions.¹⁷ However, the reverse phenomenon is reported by experimental methods as multivalent counterions limited the re-expansion due to bridging effects. One exception was reported by Hou and co-workers²⁶ in which the experimental result followed a similar trend as the theoretical prediction.¹⁷

Low molecular weight polycationic and polyanionic synthetic polymer with 100% hydrolysis were used in many of the reentrant transition studies. In this study, we have used a high molecular weight and partially hydrolyzed polyacrylamide. Characterization of high molecular weight polymer with wide distribution is very challenging work. In fact, a methodology was suggested for characterization of phase transitions of LPS as a function of Al(III) concentration in low salinity solvents in our previous work.²⁹ In the present work, we extended the scope of LPS phase transition study and attempt to validate the methodology for high saline conditions. A combination of NMR (2D NOESY and DOSY), dynamic rheology and UV–visible spectroscopy were used to investigate the phase transition of LPS as a function of Al³⁺ in a high salinity solvent.

EXPERIMENTAL

Materials and Sample Preparation

A concentrated brine (NaCl) solution was prepared by dissolving p.a. grade salts (Fluka, Riedel-de Haën) in deionized water and filtered through 0.45 μm filters (Millipore). Stock solution was diluted to the desired concentration, 5 wt % (0.850 M) NaCl.

Aluminum Citrate. A stock solution of 3000 ppm (weight Al/total weight) of aluminum citrate was prepared in 5 wt % NaCl and adjusted to neutral pH to avoid precipitation. The solution was prepared from an aluminum citrate solution (Dr. Paul Lohmann AG) which contained 8.8 wt % Al. Aluminum concentration was measured by ICP-OES (Perkin-Elmer).

Polymer and LPS. Partial hydrolyzed polyacrylamide (HPAM) polymer, Flopaam 3630S, (SNF Floerger) with an average molecular weight of 20 MDa and 25–30% degree of hydrolysis was used. A stock solution of 5000 ppm (w/w) was prepared by dispersing dry polymer granulate in 5 wt % NaCl solvent, as described by API RP 63.³⁰ The stock polymer solution was diluted to the desired concentrations of HPAM by adding 5 wt % NaCl and stirring the solution for a minimum of 24 h using a magnetic stirrer at low speed. LPS were prepared by adding a desired amount of aluminum citrate from stock solution into HPAM solutions. The pH was subsequently adjusted to 7 ± 0.1 by addition of NH₄OH and HCl. The choice of pH was based on an optimal condition found from our previous study of pH influence on LPS properties.³¹ LPS solutions were kept under slow stirring on a magnetic stirrer for three days before use to ensure that the reaction between polymer and AlCit to reach equilibrium. All samples in this study are prepared at ambient temperature.

To distinguish between HPAM and LPS formulations the following nomenclature was introduced ‘Polymer concentration_crosslinker

concentration_solvent concentration', for instance 600_20_5 is used for a solution which consists of 600 ppm HPAM and 20 ppm Al in 5 wt % NaCl solvent.

Methodology

pH Meter. All the pH of sample was measured by ISFET pH meter (Model 24309). The pH meter has a water proof nonglass probe (Model 24307), which measure with resolution of 0.01 and accuracy of ± 0.01 . The probe was calibrated with three buffer solutions (i.e., pH of 4.01, 7.00, and 10.01) before measurement was carried out.

Rheology. Rheological measurements were performed on an Anton Paar Physica MCR 300 stress-controlled rheometer. Measurements were performed at 22 °C using double gap geometry (DG 26.7). Samples were allowed to temperature equilibrate for a minimum of 5 min before starting the measurements. Amplitude sweep was performed using a frequency of 10 Hz. Strain values between 0.01 and 3000% were applied. The linear viscoelastic region (LVR) was determined and a suitable strain value was used for the frequency sweep measurements. Frequencies from 0.1 Hz to 10 were applied for frequency sweep measurements.

UV-Visible Spectroscopy. The samples were filled in 1 cm path-length quartz cuvette and an absorbance spectra were recorded on a Perkin-Elmer Lambda 25 spectrometer, between 200–700 nm. A blank sample was used for background correction with 100% transmittance.

NMR Spectroscopy. Liquid state ^1H NMR measurements were performed on a Bruker AVANCE DRX 600 NMR spectrometer. A 5 mm triple resonance (^1H , ^{13}C , and ^{15}N) inverse cryogenic probe-head with z-gradient coils and cold ^1H and ^{13}C preamplification was used for the DRX 600. The samples were prepared with 10% D_2O (99.9%, Aldrich) in 5 mm 528-PP-7 NMR tubes (Sigma Aldrich). Shimming and tuning of the samples were performed automatically. Bruker standard pulse sequences were used throughout this study. Typical acquisition parameters used for one dimensional ^1H NMR measurements were 90° pulse (18.8–20 μs), 32 number of scans, 4 dummy scans, 12 kHz spectral width and 16K number of data points. The intense water signal was suppressed using excitation sculpting.

Phase sensitive ^1H – ^1H NOESY spectra were recorded using a pulse sequence with gradient selection. The basic phenomenon responsible for NOE appearance is the crossrelaxation, which is caused by the intramolecular dipolar interaction between two nuclei. The efficiency of this crossrelaxation depends on the internuclear distance and on the rotational correlation time of the molecular motion. Several NOESY spectra were recorded with different mixing times (τ_m); 80, 100, 150, 200, 300, and 400 ms. However, the spectrum with 200 ms mixing time was analyzed in detail since this lead to the maximum value of the NOE cross peaks. The parameters used to obtain the NOESY spectra were; 90° pulse length (18.8–20 μs), 16 number of scans, 16 number of dummy scans, 2048 data points in the direct dimension and 256 data points in the indirect dimension, 9 kHz spectral width and 200 ms mixing time.

For the DOSY experiment, the water in the sample was replaced by D_2O after freeze-drying and 600 μL of the sample was placed

in an NMR tube. We used bipolar longitudinal eddy current delay (BPLED) pulse sequence, which is a modified version of the longitudinal eddy current delay (LED) sequence.³² The main advantages applying BPLED over LED, is that the effective gradient output is doubled and that eddy currents are reduced to a minimum. Hence, the BPLED pulse sequence is important to measure relatively low diffusion coefficients where large gradients are required. For each experiment, the gradient pulse length was kept constant to 2 ms, while the gradient strength varied from 1 to 52 G/cm in 32 linear steps, 32,768 data points, and 4 numbers of dummy scans. The diffusion time was 100 ms in all experiments and other spectral parameters exported from 1D ^1H experiment.

TSP [sodium 3-(trimethylsilyl) tetrauteriopropionate] was used as chemical shift reference. All experiments were carried out at 25 °C, and the spectra were processed using Bruker TopSpin 3.2.

RESULTS AND DISCUSSION

The experiments were conducted to understand the phase transition of LPS as a function of Al^{3+} concentration at high brine salinity (5 wt % NaCl). The influence of salinity can be evaluated by comparing with our previous results of LPS prepared in 0.5 wt % NaCl.²⁹ The presence of monovalent counterions influences the HPAM conformation as the counterions condense on the polymer chain and screen the electrostatic interactions between charged monomer units. Since the acrylate side chains are negatively charged at neutral pH, low concentration of counterions will reduce repulsion between charged monomer units. At intermediate counterions concentration, charges will be balanced, which promote intra- and intermolecular interactions of polymer solution. However, at high counterion concentration, the polymers re-gain their negative charges as result of overcharging and develop repulsion within or between polymer chains that leads to chain re-expansion. Addition of trivalent counterion (Al^{3+}) into this solution leads to more complex interaction as it introduce metal–ligand interplay in addition to counterion condensation. The high coordination number of Al^{3+} may promote intra- and interstrand crosslinking. This study will attempt to characterize the phase transition of LPS as a function of Al^{3+} concentration under high salinity solvent by applying dynamic rheology and different spectroscopy methods.

Conformational transitions may be observed by NMR parameters such as chemical shift, transferred nuclear overhauser effect (NOE), relaxation, and diffusion. Phase sensitive NOE (2D ^1H – ^1H NOESY) and diffusion (2D ^1H DOSY) spectra were recorded to gain information on conformational change of LPS as a function of Al^{3+} . First, 1D ^1H NMR was carried out for each sample to optimize parameters for 2D ^1H – ^1H NMR experiments. Figure 1 shows the chemical structure of HPAM and the assignment of 1D ^1H spectrum of LPS (600_20_5) shown in Figure 2.

Two-Dimensional (1H–1H) NOESY NMR

We have performed 2D ^1H – ^1H NOESY NMR experiments of LPS as a function of Al^{3+} concentration to investigate the phase transition. The dipolar couplings between the polymer backbone

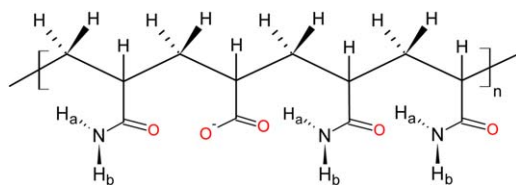


Figure 1. Chemical structure of HPAM, where the charged groups are distributed randomly. [Color figure can be viewed in the online issue, which is available at wileyonlinelibrary.com.]

protons (CH and CH₂) and amide protons (NH_a and NH_b) were used as indicator for conformational transition. Dipolar coupling between polymer backbone protons (CH and CH₂) are not possible to use because of difficult to integrate the water crosspeak signals. As expected, the dipolar coupling between the two amide protons (NH_a × NH_b) had insignificant change as Al³⁺ concentration increased. This coupling was, therefore, used as a reference for internuclear distance calculations by applying isolated spin-pair approximation.

The spectra of HPAM (600_0_5) and LPS (600_20_5) are shown in Figure 3. The box section shows the dipolar couplings between the polymer backbone protons (CH and CH₂) and amide protons (NH_a and NH_b). These two spectra superimposed and displayed at bottom of the figure. The spectra showed no NOE cross peak signals between the methylene backbone proton (CH₂) and amide protons (NH_a and NH_b). This indicates that the distances between these protons are larger than about 5 Å both in HPAM and LPS. The cross peak signals between the CH polymer backbone proton and the amide protons (NH_a and NH_b) in HPAM (600_0_5) are stronger than LPS (600_20_5). Hence, the polymer backbone (CH) and amide protons (NH_a and NH_b) cross peak signal may be used as an indicator for conformational change of LPS as a function of Al³⁺ concentration. Dipolar coupling can develop through chemical exchange in addition to crossrelaxation. However, the work by Rajamohanan and co-workers³³ showed that the cross relaxation dominate over chemical exchange at ambient temperature for amide protons, justifying the use of amide protons for NOE distance measurements.

The isolated spin-pair approximation was employed to transform NOE cross peak signal volume into distances (eq. 1). The NOE cross peak signal volume of amide protons was used as reference peak; because of change of the peak volume as a function of Al³⁺ concentration is insignificant.

$$d_{ij} = d_{ref} \cdot \sqrt[6]{\frac{V_{ref}}{V_{ij}}} \quad (1)$$

where V_{ref} and V_{ij} are the crosspeak volumes integrated from the NOESY spectrum and d_{ref} is the internal calibration distance, $NH_a \times NH_b$, $d_{ref} \approx 1.63$ Å (calculated based on bond angle). The NOESY crosspeak volumes are transformed into distances, and plotted as a function of Al³⁺ concentration, demonstrated in Figure 4. Two integrations were performed on the same spectrum and the average value is used in the plot.

In our previous study, HPAM and LPS were prepared in a low salinity (i.e., 0.5 wt % NaCl),²⁹ the distance $d_{CH_2-NH_a}$ varied between 3.0 and 4.1 Å, whereas $d_{CH_2-NH_b}$ varied between 2.4 and 2.6 Å. However, at higher salinity (5 wt % NaCl), these distances are longer than 5 Å for all concentrations of Al³⁺ (see Figure S1 in Supporting Information) and thereby, no cross peak signals. This result indicates a conformational change of the flexible polymer molecule from compact state to an extended state. The salinity increase appears to induce chain re-expansion that interpreted as reentrant conformational transition. This is further suggested by the changes observed in $d_{CH-NH_a/b}$. At lower salinity (0.5 wt % NaCl), addition of 20 and 40 ppm Al³⁺ induced reduction in $d_{CH-NH_a/b}$ by 0.3 Å, suggesting a more compact conformation. However, at high salinity (5 wt % NaCl), the opposite trend was observed in which the distances increased by 0.15 Å, see Figure 4. Furthermore, LPS formulation with 100 ppm of Al³⁺ showed maximum spatial proximity in which the chain re-expansion reached optimal condition. These results are in agreement with chain re-expansion.

However, after addition of 120 ppm Al³⁺ into HPAM solution, the spatial proximity of amide proton-backbone proton is reduced and thereby, the extent of chain re-expansion suppressed. Below 100 ppm of Al³⁺ the chain re-expansion could explain the observed increase in amide proton-backbone proton distance. The distance indifference to aluminum concentration above 100 ppm might be due crosslinking of HPAM by Al³⁺ dominating over chain re-expansion. A simple calculation consider that constant degree of hydrolysis (28%) of 600 ppm HPAM corresponds to 2.3 mM carboxylate and 100 ppm Al³⁺ corresponds to a concentration of 3.7 mM. The carboxylate:Al³⁺ ratio is 1:1.6, while the charge ratio is 1:4.8. It is, therefore, not straight forward why 100 ppm Al³⁺ appears as a transition concentration. A detailed analysis required equilibrium constants for the various aluminum species in solution, which are very difficult to obtain due to the highly complex chemistry of aluminum citrate complexes

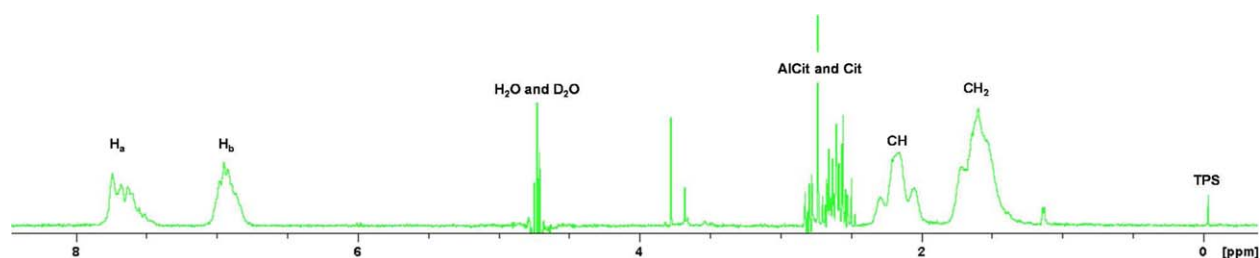


Figure 2. Assignment of ¹H NMR spectrum of LPS (600_20_5). [Color figure can be viewed in the online issue, which is available at wileyonlinelibrary.com.]

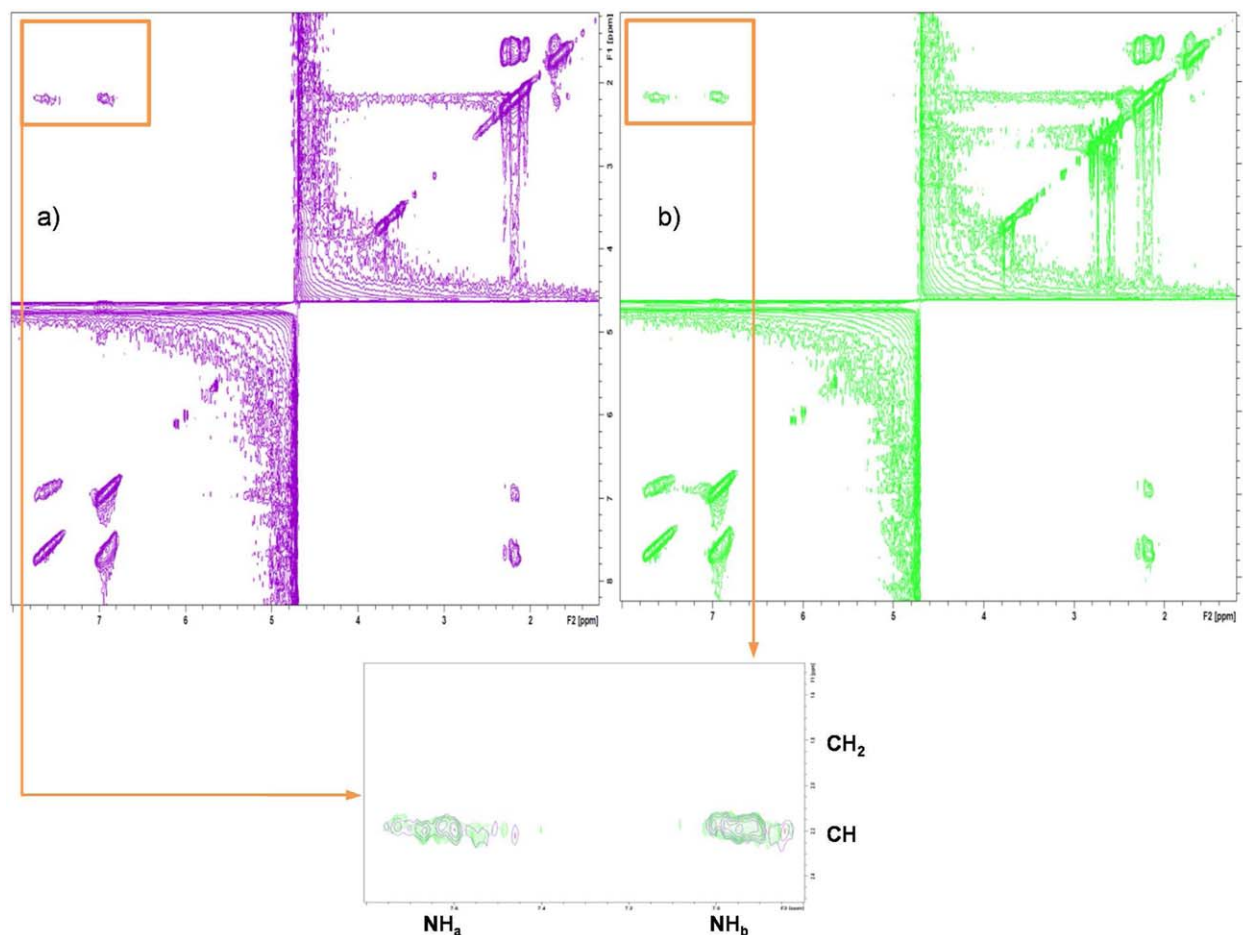


Figure 3. 2D ^1H - ^1H NOESY spectra of (a) HPAM (600_0_5) and (b) LPS (600_20_5). [Color figure can be viewed in the online issue, which is available at wileyonlinelibrary.com.]

(see e.g., Kedir *et al.*³¹ and Happel and Seubert³⁴ and references therein). It is beyond the scope of this work to evaluate the interaction of different aluminum-citrate species with polymer. Hence,

we restrained the discussion to point out that aluminum is in surplus amount at 100 ppm, and is also present as aluminum citrate species in solution. The observations from NOESY indicate that

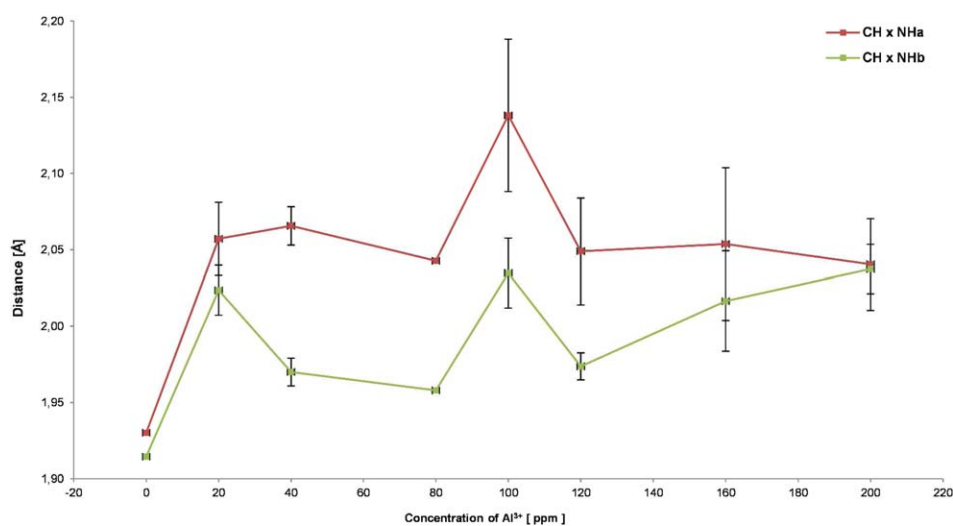


Figure 4. The distance (spatial proximity) between the backbone proton (CH) and amide protons (NH_a and NH_b) as a function of Al^{3+} concentration for 600 ppm HPAM in 5% NaCl. Points are average over two integrations; error bars show the spread between the two integrations. [Color figure can be viewed in the online issue, which is available at wileyonlinelibrary.com.]

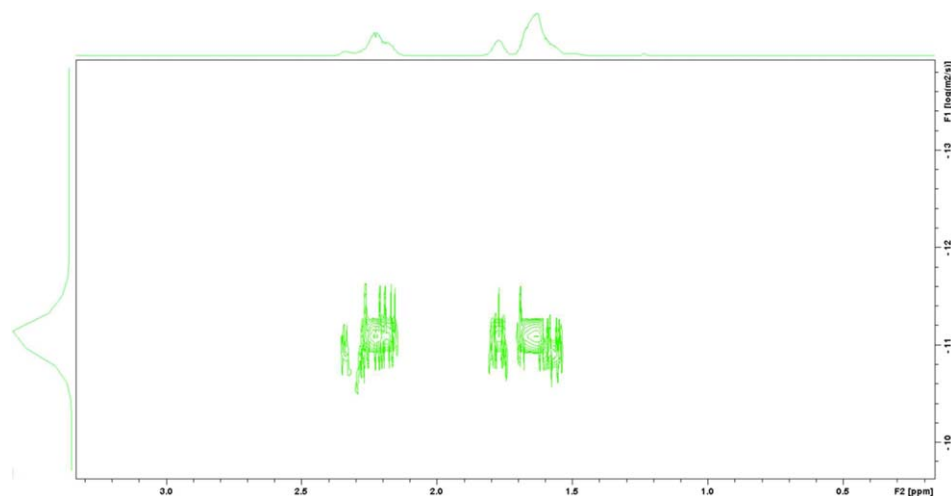


Figure 5. Diffusion coefficient distribution of LPS (600_100_0.5) from 2D ^1H DOSY spectrum, the left y axis shows the distribution curve for the diffusion of polymer backbone protons CH (downfield) and CH_2 (upfield). The top x axis shows the 1D ^1H spectrum. [Color figure can be viewed in the online issue, which is available at wileyonlinelibrary.com.]

100 ppm may be a concentration in which there is a change from primarily intermolecular to intramolecular crosslinking. Roiter *et al.*²³ and Trotsenko *et al.*²⁸ reported that chain re-expansion is limited for multivalent counterions compared to monovalent counterions due to bridging of the polymer chains by multivalent counterion. Hence, the presence of multivalent counterion (Al^{3+}) in HPAM (600_0_5) solution may result not only in chain re-expansion but also bridging or crosslinking of the HPAM coils.

Two-Dimensional ^1H DOSY NMR

We have performed diffusion ordered spectroscopy (DOSY) experiments to aid determination of conformational transitions of LPS as a function of Al^{3+} concentration. Molecules in solution travel through random translational diffusion as a result of their thermal energy. For an ideal liquid, the diffusion coefficient can be determined by the Stokes–Einstein equation as it relate to the effective size and viscosity of the molecular species. However, the diffusion coefficient of non-Newtonian liquids might be influenced by size, molecular weight, shape, viscosity, binding phenomena, and molecular interactions. In addition, determination of diffusion coefficients of polydisperse polymer solutions is more complex than monodisperse polymer solutions because of different modes of diffusion can occur.³⁵ However, the DOSY experiment is sensitive to agglomeration as significant size increase for this high molecular weight polymer.

The diffusion coefficients of D_2O , TPS, citrates, and backbone protons (CH and CH_2) were measured. However, the diffusion coefficient of backbone protons was used to examine the conformational change of LPS because of others diffusion coefficients exhibited insignificant change. In addition, diffusion coefficient of backbone protons can directly reveal the changes with regard to hydrodynamic radius and agglomeration in LPS. Figure 5 show the result of DOSY spectrum of LPS (600_100_5) sample.

The signal decay in a diffusion NMR experiment depends on the mean displacement of the molecules during a certain time, known

as the diffusion time. A polymer with high molecular weight may restrict the diffusion motion and deviate slightly from the linear relationship between the mean displacement and the diffusion time. However, relative differences in the measured diffusion coefficient can still be used to determine the phase transitions of LPS. Two parallels were measured for some of the samples and average diffusion coefficients used in Figure 6.

The diffusion coefficient of HPAM solution prepared in 5 wt % NaCl diffuse faster than HPAM solution made in 0.5 wt % NaCl ($\log D = -12.0 \text{ m}^2/\text{s}$).²⁹ This indicates that the effective hydrodynamic radius of 600 ppm HPAM is larger in 0.5 wt % NaCl, despite the re-expansion occurring at 5 wt % NaCl. Addition of 20 to 100 ppm Al^{3+} result in a steady increase in the diffusion coefficient, see Figure 6. However, the diffusion coefficients decrease for higher concentrations of Al^{3+} , indicating a change at 100 ppm Al^{3+} . The property change at 100 ppm was also observed in the NOESY result. However, the increase in diffusion coefficient cannot be easily explained by increase in re-expansion for Al^{3+} concentrations. Agglomeration appears not to be occurring as the change in diffusion coefficient would be expected to be larger due to the large increase in molecular weight. Thus, the diffusion pattern seems more complex than what can be interpreted by applying Stokes–Einstein equation.

Oscillatory Rheology

LPS is a polymer nanoparticle that has viscoelastic properties, and conformational changes influence the viscoelasticity. The conformational change of LPS as a function of Al^{3+} concentration is also investigated by oscillatory rheology. Amplitude sweep measurements were performed for each sample to determine the strain value within the linear viscoelastic region (LVE), and followed by frequency sweep measurements at the selected strain values. Two replicates were performed for each sample; the results are averaged and plotted as shown in Figures 7 and 8.

Loss factor represent the ratio of loss modulus to the storage modulus ($\tan \delta = G''/G'$), a dimensionless unit. Figure 9 shows

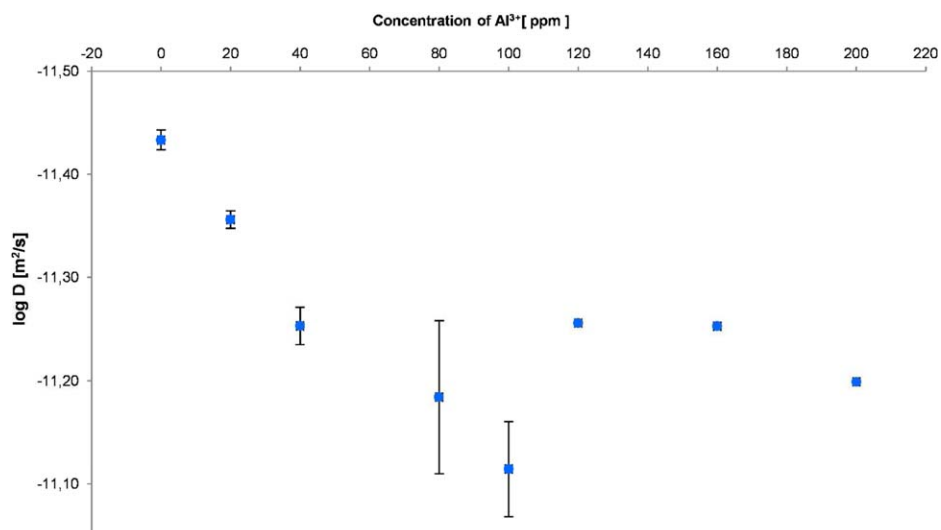


Figure 6. Diffusion coefficient of polymer backbone protons (CH and CH₂) as a function of Al³⁺ concentration. [Color figure can be viewed in the online issue, which is available at wileyonlinelibrary.com.]

the loss factor and complex viscosity at constant angular frequency (1 rad/s) for sample as a function of Al³⁺ concentration to assist the interpretation.

As seen in Figures (7 and 8), and 9, LPS formulations with Al³⁺ concentrations from 20 to 80 ppm shows increase in complex viscosity and in elasticity compared to HPAM (i.e., 600_0_5). This change can be explained by Al³⁺ induced chain re-expansion in HPAM. Loss factor independence against angular frequency is an indication for strong polymer internal structure. In Figure 7, LPS with 20 ppm of Al (III) shows that the loss factor is frequency dependent at low frequency, suggests that the internal structure is weaker compared to HPAM. The formulation of LPS with 40 and 80 ppm Al³⁺ shows the loss factor is independent of angular frequency in the same region suggest that increase of Al³⁺ concentration restrengthen the polymer internal structure.

Addition of 100 ppm of Al³⁺ appeared to be a changing the trend as it observed in NOESY experiments. In this LPS (600_100_5), the loss factor is frequency independent at high frequencies and the complex viscosity show much less shear thinning than HPAM or other LPS formulations (Figure 7). These observations suggest more physical interactions between polymer coils because of chain re-expansion in which the expansion reached maximum. At 120 and 160 ppm of Al³⁺ concentration, LPS regain elasticity, but shows decrease in complex viscosity, seen in Figures 7–9. This may be explained by intramolecular crosslinking of HPAM by Al³⁺, which strengthen polymer internal structure and reduce effective hydrodynamic radius. Addition of 200 ppm Al³⁺ into HPAM leads to increase the loss factor due to loss of elasticity and lowers the complex viscosity. This might be due to the balance competition between the chain re-expansion and intramolecular crosslinking of HPAM by Al³⁺ that weaken the polymer internal structure.

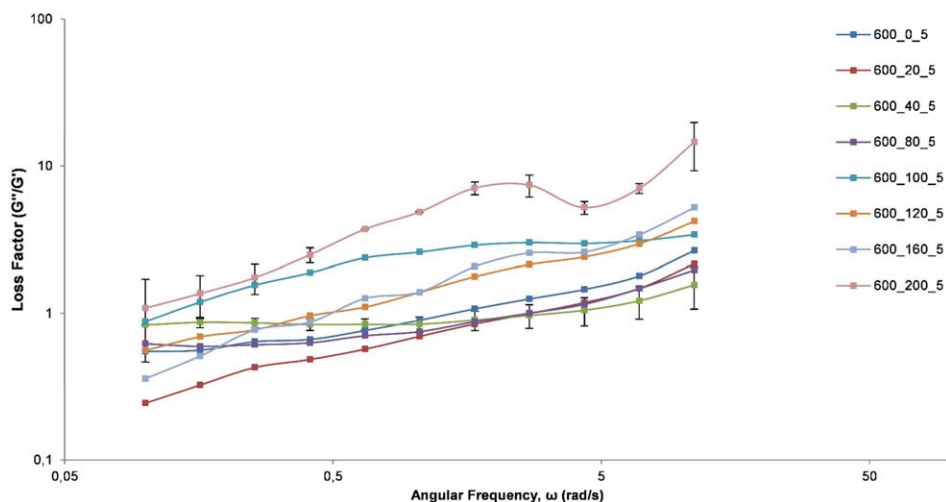


Figure 7. Loss factor (G''/G') as a function of angular frequency for HPAM and LPS. Error bars are not shown for some points to improve figure readability. [Color figure can be viewed in the online issue, which is available at wileyonlinelibrary.com.]

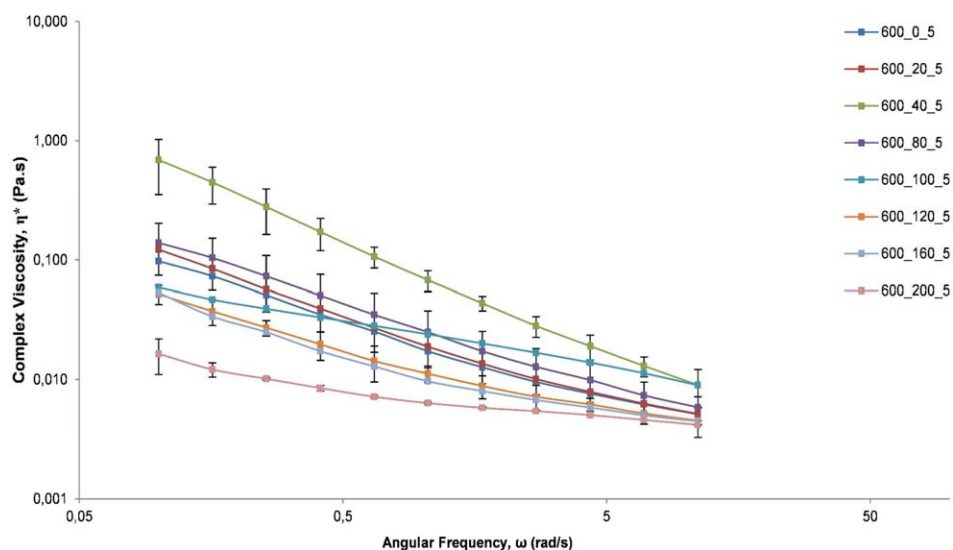


Figure 8. Complex viscosity as a function of angular frequency for HPAM and LPS. Error bars are not shown for some points to improve figure readability. [Color figure can be viewed in the online issue, which is available at wileyonlinelibrary.com.]

In summary, addition of Al^{3+} to HPAM at 5 wt % NaCl induces chain expansion at concentrations up to 100 ppm Al^{3+} . The chain re-expansion is shown by increase in complex viscosity and elasticity. Above 100 ppm Al^{3+} reduction in complex viscosity without a large increase in elasticity indicate intramolecular crosslinking of HPAM by Al^{3+} while the reentrant transition occurs. These observations are in good agreement with the pattern observed from NOESY experiments.

UV-Visible Spectroscopy

The reentrant phase transition was investigated using UV-visible spectroscopy. The result of HPAM and LPS UV absorbance measurements show insignificant differences, and we were unable to attribute the conformational changes regarding with chain re-expansion. However, the concept of

reentrant phase transition is investigated with high concentration polymer solutions at low and high brine salinity. Thus, 5000 ppm polymer solutions were prepared in 0.5 and 5% NaCl.

Figure 10 shows the average value of the absorbance measured in the range of UV-visible spectra showed at bottom left. The result shows that the absorbance is decreased as brine salinity increases from 0.5 to 5 wt % in 5000 ppm polymer solution. This may indicate that the polymer solution in 0.5 wt % NaCl exists in coiled state and absorbs more UV light. However, the increase in brine salinity changes the polymer conformation and decrease the UV absorbance as result of reentrant transition. Similar results were observed for reentrant transition of protein study by Zhang and co-workers.³⁶

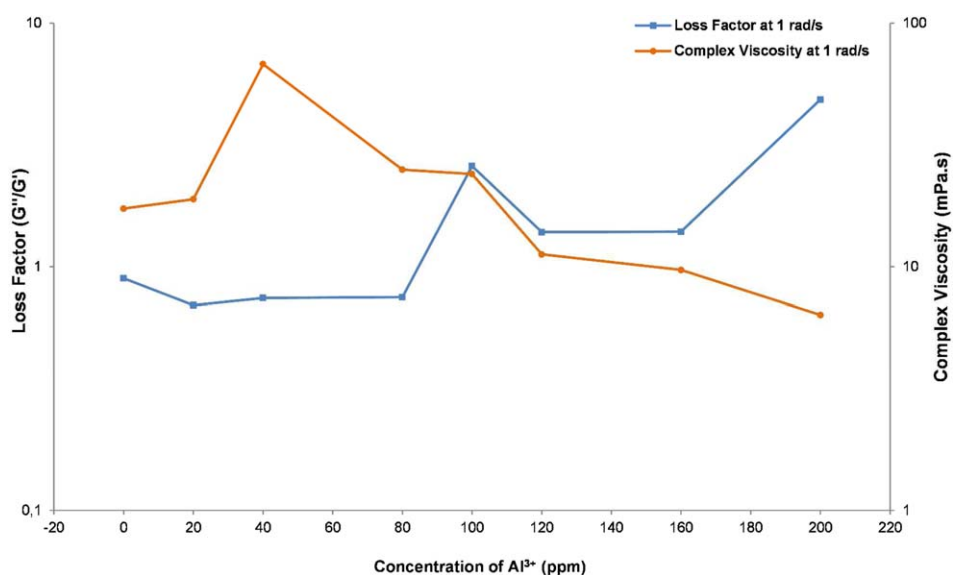


Figure 9. Loss factor and complex viscosity of LPS as a function of Al^{3+} concentration at 1 rad/s. [Color figure can be viewed in the online issue, which is available at wileyonlinelibrary.com.]

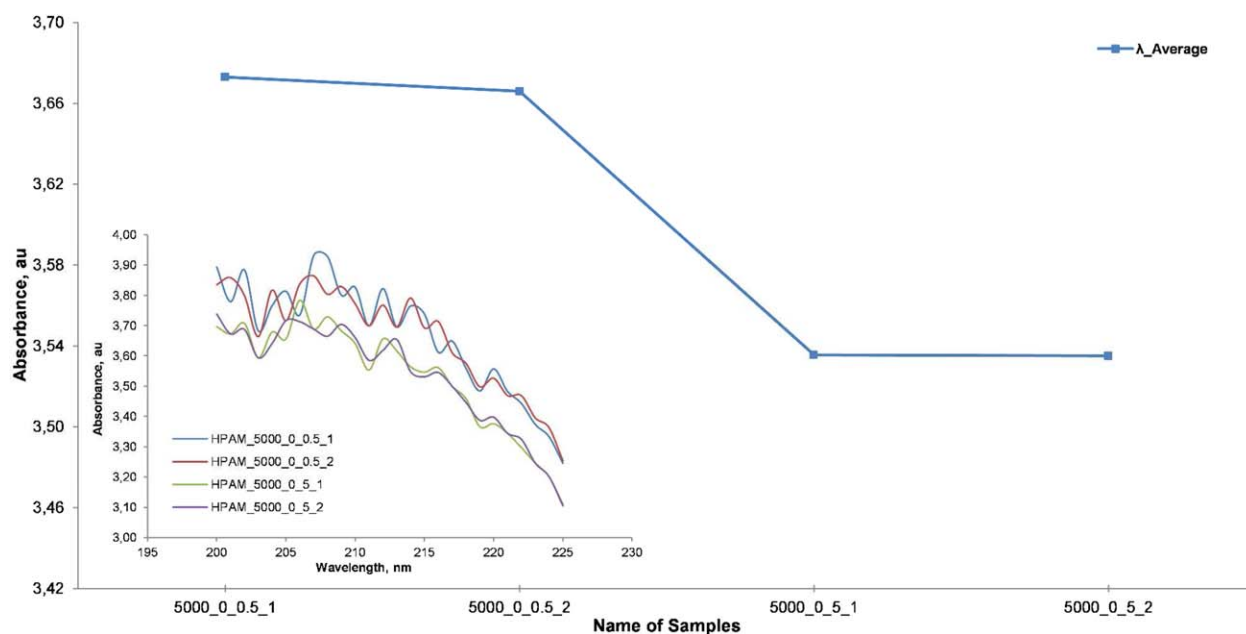


Figure 10. UV–visible absorbance of 5000 ppm HPAM polymer in 0.5 and 5 wt % NaCl measured between 200 and 700 nm. Insert figure show UV spectrum from 200 to 225 nm. [Color figure can be viewed in the online issue, which is available at wileyonlinelibrary.com.]

In summary, the combined methods were used to investigate reentrant phase transitions of LPS as a function of Al^{3+} under high salinity solvent. Two-dimensional NOESY NMR was used to acquire structural changes and indirectly measures the effective hydrodynamic radii. Dynamic rheology, diffusion NMR and UV–visible spectroscopy were also used to measure viscoelasticity, apparent diffusion coefficient and optical properties, respectively.

The result of 2D NOESY experiment exhibited that the dipolar coupling between backbone protons (CH_2) and amide protons (NH_a and NH_b) was much weaker than in low salinity solvent.

This indicates that the spatial proximity between these protons was larger under high salinity and therefore, HPAM present in the state of chain re-expansion or reentrant transition. UV–visible spectra also confirmed the reentrant transition of HPAM at high salinity solvent (5 wt % NaCl) by decreasing the absorbance compared to low salinity solvent (0.5 wt % NaCl). Addition of Al^{3+} from 20 to 100 ppm into HPAM led to further increase of their spatial proximity indicates that Al^{3+} induced reentrant transition. This trend was confirmed by oscillatory rheology, which showed an increase of elasticity and complex

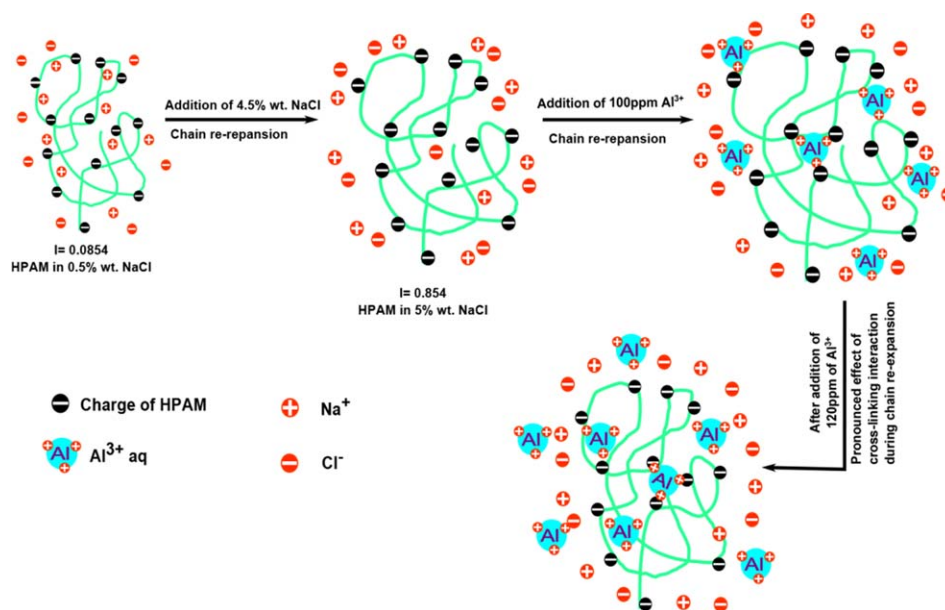


Figure 11. A schematic illustration of phase transition of LPS as a function of Al^{3+} concentration at high salinity solvent. [Color figure can be viewed in the online issue, which is available at wileyonlinelibrary.com.]

viscosity for the same concentrations of Al^{3+} , both indicating chain re-expansion. Finer analysis showed subtle differences within the same range. The LPS with 20 ppm of Al^{3+} showed a relatively weaker internal structure compared to LPS with 40 and 80 ppm as seen by the frequency dependent loss factor at low frequencies. LPS with 40 ppm of Al^{3+} exhibited the highest complex viscosity and elasticity possibly due to the expanded chains has strong internal structure.

All methods show that there is a change in behavior for LPS with 100 ppm of Al^{3+} . NOESY spectra indicate that the reentrant transition reach maximum at this concentration and oscillatory rheology shows a significant loss of elasticity, but complex viscosity is relatively high. Both loss factor and complex viscosity curves are significantly different for LPS with 100 ppm Al^{3+} than for higher or lower concentrations. In addition, the diffusion constant changes at this concentration, diffusion being fastest for 100 ppm Al^{3+} LPS. Further increasing the concentration to 120 and 160 ppm of Al^{3+} leads to a decrease in complex viscosity and increase in elasticity. This suggests that Al^{3+} is crosslinking the acrylate side chains that compact and regain the strength of internal structure. The diffusion coefficient is slightly reduced and may not occur intermolecular binding that gives a weak gel network. In addition, at high salinity, intermolecular crosslinking of HPAM by Al^{3+} might be energetically unfavorable at this polymer concentration. It is, therefore, most likely that the increased concentration led to intramolecular crosslinking of HPAM by Al^{3+} . This is in agreement with NOESY experimental observation in which the spatial proximity between amide-backbone protons is reduced. Figure 11 is a sketch of phase transition of LPS at high salinity solvent, which illustrates the overall experimental observation.

CONCLUSIONS

Linked polymer solution (LPS) was prepared from high molecular weight ($>10 \times 10^6$ Da), low concentration (<1000 ppm), polydisperse solutions of HPAM, using Al^{3+} as a crosslinker in a high salinity solvent. Characterization of phase transitions of LPS is highly complex and challenging, primarily due to distributions of multiple species present in solution. These are still limitations in which LPS have shown oil mobilization potential. A single characterization method is insufficient and thus, we have applied a combinatorial method that made it possible to rationalize the dominating species and reentrant transition of HPAM as a function Al^{3+} at high salinity solvent. By applying this method, we observed that at 5 wt % NaCl solvent, HPAM was in re-expanded state. Addition of aluminum counterion induced further chain re-expansion up to a threshold concentration, observed to be 100 ppm of Al^{3+} . However, further addition of Al^{3+} (i.e., >100 ppm) led to suppressed the rate of chain re-expansion, possible because of intramolecular crosslinking of HPAM by Al^{3+} dominating over chain re-expansion. In this re-entrant transition process, intermolecular crosslinking reaction was not observed. Chain re-expansion of polyelectrolytes is often concluded based on viscosity increase as a function of salinity. However, the combination of NMR and rheology data showed that the polymer underwent chain re-expansion while the relative viscosities of LPS decreased. This may be

explained by weak strength of the polymer internal structure. Therefore, it is important to closely investigate the strength of polymer internal structure and apply several experimental methods when evaluating chain re-expansion.

ACKNOWLEDGMENTS

The authors acknowledge the Norwegian Research Council (NFR) for financial support through the PETROMAKS program.

REFERENCES

1. Spildo, K.; Skauge, A.; Aarra, M. G.; Tveheyo, M. T. *SPE Reserv. Eval. Eng.* **2009**, *12*, 427.
2. Li, M. Y.; Lin, M. Q.; Zheng, X. Y.; Wu, Z. L. *Oilfield Chem.* **2000**, *17*, 144.
3. Shiyi, Y.; Dong, H.; Qiang, W.; Hua, Y. Numerical Simulator for the Combination Process of Profile Control and Polymer Flooding. Paper SPE64792 presented at the *SPE International Oil and Gas Conference and Exhibition in China held in Beijing, China*, 7–10 November, **2000**.
4. Wang, W.; Lu, X. *Pet. Sci. Technol.* **2009**, *27*, 699.
5. Xie, C.; Guan, Z.; Blunt, M.; Zhou, H. *J. Can. Pet. Technol.* **2009**, *48*, 37.
6. Sing, C. E.; Zwanikken, J. W.; Olvera de la Cruz, M. *Macromolecules* **2013**, *46*, 5053.
7. Dobrynin, A. V.; Rubinstein, M. *Prog. Polym. Sci.* **2005**, *30*, 1049.
8. Nguyen, T. T.; Rouzina, I.; Shklovskii, B. I. *J. Chem. Phys.* **2000**, *112*, 2562.
9. Nguyen, T. T.; Shklovskii, B. I. *J. Chem. Phys.* **2001**, *115*, 7298.
10. Lee, S.; Le, T. T.; Nguyen, T. T. *Phys. Rev. Lett.* **2010**, *105*, 248101.
11. Sennato, S.; Bordini, F.; Cametti, C.; Diociaiuti, M.; Malaspina, P. *Biochim. Biophys. Acta Biomembr.* **2005**, *1714*, 11.
12. Roosen-Runge, F.; Heck, B. S.; Zhang, F.; Kohlbacher, O.; Schreiber, F. *J. Phys. Chem. B* **2013**, *117*, 5777.
13. Zhang, F.; Wegler, S.; Ziller, M. J.; Ianeselli, L.; Heck, B. S.; Hildebrandt, A.; Kohlbacher, O.; Skoda, M. W. A.; Jacobs, R. M. J.; Schreiber, F. *Proteins Struct. Funct. Bioinform.* **2010**, *78*, 3450.
14. Solis, F. J.; Olvera de la Cruz, M. *Eur. Phys. J. E: Soft Matter Biol. Phys.* **2001**, *4*, 143.
15. Solis, F. J. *J. Chem. Phys.* **2002**, *117*, 9009.
16. Nguyen, T. T.; Shklovskii, B. I. *J. Chem. Phys. A* **2001**, *293*, 324.
17. Hsiao, P. Y.; Luijten, E. *Phys. Rev. Lett.* **2006**, *97*, 148301.
18. Hsiao, P. Y. *J. Phys. Chem. B* **2008**, *112*, 7347.
19. Kundagrami, A.; Muthukumar, M. *J. Chem. Phys.* **2008**, *128*, 2449011 244901.
20. Jha, P. K.; Zwanikken, J. W.; Olvera de la Cruz, M. *Soft Matter* **2012**, *8*, 9519.
21. Nguyen, T. T.; Grosberg, A.; Yu, S. B. I. *J. Chem. Phys.* **2000**, *113*, 1110.

22. Jan, J. S.; Breedveld, V. *Macromolecules* **2008**, *41*, 6517.
23. Roiter, Y.; Trotsenko, O.; Tokarev, V.; Minko, S. *J. Am. Chem. Soc.* **2010**, *132*, 13660.
24. Olvera de la Cruz, M.; Belloni, L.; Delsanti, M.; Dalbiez, J. P.; Spalla, O.; Drifford, M. *J. Chem. Phys.* **1995**, *103*, 5781.
25. Jia, P.; Zhao, J. *J. Chem. Phys.* **2009**, *131*, 2311031.
26. Hou, Y.; Liu, G.; Wu, Y.; Zhang, G. *Phys. Chem. Chem. Phys.* **2011**, *13*, 2880.
27. Dubois, E.; Boué, F. *Macromolecules* **2001**, *34*, 3684.
28. Trotsenko, O.; Roiter, Y.; Minko, S. *Langmuir* **2012**, *28*, 6037.
29. Kedir, A. S.; Seland, J. G.; Skauge, A.; Skauge, T. *Energy Fuels* **2014**, *28*, 2948.
30. API RP 63. Recommended Practices for Evaluation of Polymers Used in Enhanced Oil Recovery Operations, 1st ed.; American Petroleum Institute: Washington, DC, **1990**, p 86.
31. Kedir, A. S.; Seland, J. G.; Skauge, A.; Skauge, T. *Energy Fuels* **2014**, *28*, 2343.
32. Wu, D. H.; Chen, A. D.; Johnson, C. S. *J. Magn. Reson. Ser. A* **1995**, *115*, 260.
33. Rajamohanan, P. R.; Ganapathy, S.; Ray, S. S.; Badiger, M. V.; Mashelkar, R. A. *Macromolecules* **1995**, *28*, 2533.
34. Happel, O.; Seubert, A. *J. Chromatogr. A* **2006**, *1108*, 68.
35. Walderhaug, H.; Söderman, O.; Topgaard, D. *Progr. Nucl. Magn. Res. Spectr.* **2010**, *56*, 406.
36. Zhang, F.; Skoda, M. W. A.; Jacobs, R. M. J.; Zorn, S.; Martin, R. A.; Martin, C. M.; Clark, G. F.; Weggler, S.; Hildebrandt, A.; Kohlbacher, O.; Schreiber, F. *Phys. Rev. Lett.* **2008**, *101*, 148101.